Porphyrin Depth in Lipid Bilayers as Determined by Iodide and Parallax Fluorescence Quenching Methods and Its Effect on Photosensitizing Efficiency

Irena Bronshtein,* Michal Afri,† Hana Weitman,* Aryeh A. Frimer,† Kevin M. Smith,‡ and Benjamin Ehrenberg*
*Department of Physics, †Department of Chemistry, Bar Ilan University, Ramat Gan, Israel; and ‡Department of Chemistry, Louisiana State University, Baton Rouge, Louisiana

ABSTRACT Photosensitization by porphyrins and other tetrapyrrole chromophores is used in biology and medicine to kill cells. This light-triggered generation of singlet oxygen is used to eradicate cancer cells in a process dubbed "photodynamic therapy," or PDT. Most photosensitizers are of amphiphilic character and they partition into cellular lipid membranes. The photodamage that they inflict to the host cell is mainly localized in membrane proteins. This photosensitized damage must occur in competition with the rapid diffusion of singlet oxygen through the lipid phase and its escape into the aqueous phase. In this article we show that the extent of damage can be modulated by employing modified hemato- and protoporphyrins, which have alkyl spacers of varying lengths between the tetrapyrrole ring and the carboxylate groups that are anchored at the lipid/water interface. The chromophore part of the molecule, and the point of generation of singlet oxygen, is thus located at a deeper position in the bilayer. The photosensitization efficiency was measured with 9,10-dimethylanthracene, a fluorescent chemical target for singlet oxygen. The vertical insertion of the sensitizers was assessed by two fluorescence-quenching techniques: by iodide ions that come from the aqueous phase; and by spin-probe-labeled phospholipids, that are incorporated into the bilayer, using the parallax method. These methods also show that temperature has a small effect on the depth when the membrane is in the liquid phase. However, when the bilayer undergoes a phase transition to the solid gel phase, the porphyrins are extruded toward the water interface as the temperature is lowered. These results, together with a previous publication in this journal, represent a unique and precedental case where the vertical location of a small molecule in a membrane has an effect on its membranal activity.

INTRODUCTION

Light absorption by porphyrins, phthalocyanines, and other tetrapyrrole-based molecules leads to photosensitized generation of singlet oxygen. The mechanisms by which singlet oxygen is generated and deactivated have been extensively reviewed (Schweitzer and Schmidt, 2003; DeRosa and Crutchley, 2002; Bonnett, 2002). The efficiency of singlet oxygen generation by these molecules, combined with the important attribute of their preferential uptake by cancer tissues, are the basis for photodynamic therapy (PDT), a new modality of treating malignant tumors. Several review articles on this method have recently appeared (Pandey, 2000; Ackroyd et al., 2001; Allen et al., 2001; MacDonald and Dougherty, 2001; Dougherty, 2002; Smith and Hahn, 2002). PDT is currently approved for use in specific types of malignancies in several countries around the world.

Lipophilic sensitizers that are added to liposomes or cells partition efficiently into the external lipid bilayer and, in cells, they eventually also diffuse to the membranes which envelope intracellular organelles. The more hydrophilic photosensitizers enter cells by endocytotic active mechanisms and are eventually located in polar regions in the cell. The damage that singlet oxygen causes in the cells, especially with hydrophobic sensitizers, is inflicted upon various membrane proteins (Berg and Moan, 1997; Ehrenberg et al., 1993). These lead to permeation of the membranes, electric depolarization, apoptosis, or necrosis of the cancer cells (Paardekooper et al., 1992; Oleinick et al., 2002; Kessel and Luo, 2001; Fabris et al., 2001; Moor, 2000).

The advantageous localized damage exerted by photosensitizers is a result of their selective uptake in the tumor, the localized illumination and the short range that singlet oxygen diffuses before it decays (Moan, 1990). In fact, singlet oxygen does not live out its natural lifetime in the lipid environment, which was found to be 13–35 μs (Ehrenberg et al., 1998), because it diffuses rapidly out of the membrane. Using the Einstein-Smoluchovsky diffusion equation and an oxygen diffusion coefficient of 4.7×10^{-5} cm^2/s (Fischkoff and Vanderkooi, 1975), the time it takes oxygen to traverse a root mean-square distance of 40 Å, the thickness of the bilayer, is ~2 ns. Once a singlet oxygen

Submitted February 11, 2004, and accepted for publication April 30, 2004.

Address reprint requests to B. Ehrenberg, Dept. of Physics, Bar Ilan University, Ramat Gan 52900, Israel. Tel.: 972-3-531-8427; Fax: 972-3-535-3298; E-mail: ehren@mail.biu.ac.il.

Aryeh A. Frimer is the incumbent of the Ethel and David Resnick Chair in Active Oxygen Chemistry.

Benjamin Ehrenberg is the incumbent of the Falk Chair in Laser Phototherapy.

Abbreviations used: DMA, 9,10-dimethylantracene; DMPC, dimyristoyl phosphatydilcholine; DOPC, dioleoyl phosphatydilcholine; HP, hematoporphyrin; PDT, photodynamic therapy; PP3, protoporphyrin IX; TempoPC, 1,2-dioleoyl-*sn*-glycero-3-phosphotempocholine; 5- or 12- SLPC, 1-palmitoyl-2-(5- or 12-doxyl)-stearoyl-*sn*-glycero-3-phosphocholine.

0006-3495/04/08/1155/10 $2.00

doi: 10.1529/biophysj.104.041434

molecule crosses into the aqueous medium, its lifetime becomes very short (~3 μs). Thus, a very efficient reaction must occur between singlet oxygen and its target in the lipid membrane to compete with the rapid escape from the bilayer.

In the present study we demonstrate that the critical importance of the fast diffusion of oxygen in a membrane can be employed to increase the observed photosensitized peroxidative damage of a chemical target in the membrane. This is achieved by employing two series of derivatives of protoporphyrin and hematoporphyrin, which were modified in a way that places the tetrapyrrole core in deeper locations within the membrane. Thus, the point at which singlet oxygen is generated is deeper, which extends the duration over which singlet oxygen can exert damage while diffusing, or percolating, through the lipid phase. In previous work, we demonstrated the feasibility of this approach in a limited case of protoporphyrins (Lavi et al., 2002). In the present study we show that this is indeed an approach that can be used in additional molecules as well. We have assessed the vertical depth of the porphyrins in the membranes by quenching their fluorescence in liposomes by extramembranal iodide ions, or by intramembranal spin-labeled lipids using the parallax method (Chattopadhyay and London, 1987). We also show the effect of temperature and physical phase of the lipid on the vertical displacement of the porphyrins in the bilayer.

The seminal article by Borochov and Shinitzky (1976) demonstrated the critical importance of the vertical displacement of membrane-bound and membrane-spanning proteins. Hundreds of studies followed this publication, demonstrating the effects of membrane properties, mainly its microviscosity, and membrane additives on the exposure of the protein to the lipid/water interface. This exposure can be crucial to the presentation of cellular antigens, to binding of receptors, to lateral movement of proteins and their interactions and to other effects (Shinitzky, 1984). For low molecular weight solutes it was shown that an increase of lipid viscosity tends to lead to lowered partitioning. Nevertheless, to the best of our knowledge, there has not been a demonstration of a clearcut example, besides our previous article (Lavi et al., 2002), in which the vertical location of a small molecule in a lipid bilayer had consequences on its mechanism or activity. Our current results demonstrate that in the case of photosensitization, depth has relevance to efficiency, and it can be modulated by temperature and phase of the bilayer. These results may well help in finding optimal conditions to be used in cellular photosensitized reactions and could be considered in drug design for PDT.

MATERIALS AND METHODS

Chemicals and sample preparation

Protoporphyrin IX and hematoporphyrin IX were obtained from Sigma (St. Louis, MO). The other protoporphyrin and hematoporphyrin derivatives, with alkyl carboxylate groups containing 2, 5, or 7 carbon atoms in each chain (Fig. 1), were synthesized for this project. These syntheses were

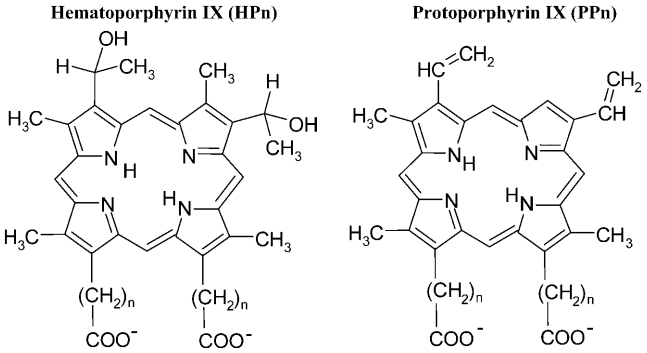

FIGURE 1 Chemical structures of HP3, PP3, and their modified analogs.

accomplished from monopyrroles using the a,c-biladiene route (Smith, 2000). 2-Formyl-3,5-dimethylpyrroles bearing 4-ester side-chains with different numbers of chain methylenes ($n = 1,4,6$) were individually reacted with the same dipyrromethane to afford the corresponding a,c-biladiene salts; these were then cyclized using the copper(II) oxidation procedure (Smith, 2000). Full experimental details of the syntheses are available (Holmes, 1997). All synthetic porphyrins were fully characterized using spectrophotometry, proton NMR spectroscopy, and elemental analysis and/or high resolution mass spectrometry. None showed evidence of any impurities. The proto- and hematoporphyrins are named HP2, PP2, HP3, PP3, HP5, PP5, and HP7, PP7, where the digit corresponds to the total number of carbon atoms in each of the two side chains.

Nitroxide-labeled PCs were purchased from Avanti Polar Lipids (Alabaster, AL). The concentration of the nitroxide was assayed by fluorescence quenching of 2-AS and 12-AS (Abrams and London, 1993). L-α-phosphatidylcholine (L-α-lecithin), dioleoylphosphatidylcholine (DOPC), and dimyristoylphosphatidylcholine (DMPC) were obtained from Sigma (St. Louis, MO). Lecithin, type XIII-E from egg yolk (99%, solution of 100 mg per ml ethanol), was a mixture of lipids with the following fatty acid makeup: 33% palmitic (C16:0), 13% stearic (C18:0), 31% oleic (C18:1), and 15% linoleic (C18:2).

$Na_2HPO_4 \cdot 12H_2O$ was acquired from Riedel-de Haën (Seelze, Germany); citric acid, *n*,*n*-dimethylformamide (DMF) and $Na_2S_2O_3$ were obtained from Frutarom (Haifa, Israel); diethyl ether (>99.8%) was purchased from Fluka Chemie (Buchs, Switzerland); 9,10-dimethylanthracene (DMA) was obtained from Sigma; potassium iodide (KI) was received from Merck (Darmstadt, Germany).

DMF stock solutions of the porphyrins [1 mM] and DMA [2 mM] were prepared, from which samples containing porphyrins at a final concentration of 0.3 μM were made up. Citrate-phosphate buffer, pH = 6.6, was used to prepare stock solutions of KI [8 M] and $Na_2S_2O_3$ [0.2 M]. KCl, up to a concentration of 0.15 M, was added to these buffer solutions to keep the ionic strength constant.

Liposome preparation

The lipid was layered at the bottom of a vial by evaporating the chloroform solvent under nitrogen. Diethyl ether was added and the solution was thoroughly re-evaporated. After addition of buffer, the sample was vortexed for 3 min and then probe-sonicated (MSE, Crawley, UK) for 15 min at 4°C until a clear solution was obtained. This suspension was used as the liposome stock solution. For the parallax measurements the lipids were composed of DOPC (or DMPC) and spin-labeled lipid at an 85:15 molar ratio. Multilamellar liposomes were prepared as above with vortexing and without sonication.

Hematoporphyrins were added from a dimethylformamide stock solution, keeping the final organic volume at <1% of the total volume. The binding to liposomes reached equilibrium within several minutes. The

protoporphyrins were added to the liposome-containing samples and were mixed on a shaker for 6 h to reach full binding equilibrium. This was tested by following the spectral changes that occur upon partitioning into the lipid layer, namely increase and shift of fluorescence, which leveled off after this time. For fluorescence quenching experiments, KI was added to the suspension of porphyrin-containing liposomes, which also contained $Na_2S_2O_3$ (at 10^{-5} M), to prevent production of colored I_2 by the oxidation of iodide.

Spectroscopic measurements

Absorption spectra were recorded on a Perkin-Elmer (Norwalk, CT) Lambda-9 UV-visible-near-IR, computer-controlled spectrophotometer. Fluorescence excitation and emission spectra and fluorescence time-drive measurements were performed on a Perkin-Elmer LS-50B digital fluorimeter. All samples had a low optical density (<0.05) at the wavelength of excitation, to maintain a linear dependence of the fluorescence intensity on concentration.

Temperature-controlled measurements

For temperature-controlled measurements we used a refrigerated circulating bath (model RTE110, Neslab Instruments, Newington, NH). We controlled the sample's temperature by pumping the temperature-controlled water through the cuvette holder in the fluorimeter. The temperature in the cuvette was measured before and after every experiment to make sure it was constant through the duration of the experiment.

Measurements of binding constants

To determine the incubation time required to reach equilibrium, the partitioning kinetics of the porphyrins into liposomes were studied for each case before measurement of the binding constant by a fluorescence time-drive measurement. The binding constant, K_b, of each porphyrin to liposomes was measured spectroscopically. K_b is defined as $K_b = [P_{bound}]/([P_{aqueous}]\times[L])$, where $[P_i]$ is the concentration of the membrane-partitioned, and aqueously dissolved, porphyrin, and $[L]$ is the concentration of the lipid. K_b is thus given in units of [lipid concentration]$^{-1}$. For each porphyrin, after each addition of an aliquot of lipid from the same batch, emission spectra were recorded, after the incubation time. For studies with liposomes, the fluorescence was excited at 402 nm and emission was measured at 626 nm.

Fluorescence quenching measurements by iodide ions

A set of samples was prepared for each porphyrin derivative. In each set the samples contained 10^{-7} M of the sensitizer, buffer at pH = 6.6, 10^{-5} M of $Na_2S_2O_3$, and increasing concentrations of KI (0–0.25 M). The fluorescence emission spectra in buffer were measured for each sample, $\lambda_{ex} = 396$ nm, $\lambda_{em} = 617$ nm. For the measurements of fluorescence quenching of HP derivatives bound to liposome, a 500-μl aliquot of solution was taken from each sample in the abovementioned set and 500 μl of lipid was added; the total concentration of the lipid in each sample was 0.4 mg/ml, which was adequate to establish complete binding of the porphyrin. The fluorescence emission spectra were measured after the incubation time.

Fluorescence quenching by spin-labeled phospholipids (Parallax method)

Samples containing sensitizer (2 μM), spin-labeled PCs, and DMPC (or DOPC) were dried under nitrogen and then under vacuum for at least 1 h; then 990 μl of buffer, pH = 6.6, and 10 μl ethanol were added and each sample was vortexed for 45 s to disperse the lipid (London and Feigenson, 1981; Kachel et al., 1995). The concentration ratio between DMPC and spin-labeled PCs in the sample was 85:15. The quenching of the porphyrin's fluorescence with each one of the spin-labeled quenchers was registered. Fluorescence spectra were measured with $\lambda_{ex} = 404$ nm, $\lambda_{em} = 626$ nm. The background was subtracted from the spectra by the data analysis software, Origin (Microcal Software, Northampton, MA). Three identical samples were prepared for each quenching measurement and the quenching data were averaged.

Effect of temperature on fluorescence quenching by spin-labeled phospholipids

The samples were prepared as described in the previous paragraph. The fluorescence was read after the sample was incubated in the fluorimeter for 2 min at the appropriate temperature; the temperature in the cuvette was regulated by the refrigerated circulation bath. The fluorescence spectra of each preparation were measured at various temperatures in the range 5°–45°C. For each experiment, triplicate samples were prepared, and the results presented below are averages of three such experiments. All fluorescence spectra were transferred to Origin for background subtraction and analysis.

Photosensitization

For the measurements of singlet oxygen quantum yields of the HP derivatives, we used the 501-nm line of an Ar^+ laser (model 2060-SR, Spectra-Physics, Mountain View, CA) as the irradiation source. The sample solution contained liposome-bound porphyrins and DMA (5 μM), which was used as a chemical target for singlet oxygen. DMA reacts selectively with singlet oxygen to form the nonfluorescent 9,10-endoperoxide with a very high rate constant (2×10^7–9×10^8 M^{-1}) in many organic solvents, as well as water (Corey and Taylor, 1964; Usui, 1973; Wilkinson and Brummer, 1981; Wilkinson et al., 1995). From our previous study (Lavi et al., 2002) it was evident that DMA is not located in a preferential depth in the membrane, unlike its ionic analog, 9-anthracenepropionic acid, which anchors at the lipid/water interface with its charged carboxylate group. The sample was stirred magnetically to obtain uniform irradiation of the whole sample contents. Irradiation of the sample was carried out in situ in the fluorimeter. The laser beam illuminated the sample cuvette along its long axis, at 90° to the direction of the excitation and emission channels of the fluorimeter. The laser power (~10 mW) at the irradiation wavelength was measured at the sample surface with a power meter (model PD2-A, Ophir, Israel), before and after the measurements, to be sure that the power remained constant during the experiment. The time-dependent fluorescence intensity of DMA was measured ($\lambda_{ex} = 375$ nm, $\lambda_{em} = 436$ nm) while the sample was illuminated by the laser. Since the fluorimeter measures a fluorescence signal that is phaselocked with the modulated light source, the presence of a CW laser beam does not interfere with the fluorescence signal. The absorbance was kept below 0.05 optical density units at the wavelength where DMA was excited. This assured a linear relationship between the concentration of DMA and its fluorescence. The fluorescence traces were then transferred to Origin for graphic and curve-fitting analyses. Under our illumination conditions, no self-sensitization, or bleaching, of any porphyrin was observed.

RESULTS

Liposome binding constants

The assessment of the binding of the porphyrins to lipid membranes was based on the pronounced spectral changes that are observed upon transfer of a porphyrin molecule from an aqueous phase to the lipid phase. We traced the change in

the intensity and shape of the fluorescence that, due to its sensitivity, enabled us to employ and measure submicromolar concentrations of the dyes, to avoid aggregation phenomena. The equation used to evaluate the binding constant of the porphyrins to liposomes, K_b (Roslaniec et al., 2000; Ehrenberg, 1992), was

$$F = \frac{F_{init} + F_{comp}K_b[L]}{1 + K_b[L]}, \quad (1)$$

where F_{init} is the fluorescence intensity measured in absence of lipid; F is the intensity measured in the presence of lipid at concentration $[L]$; and F_{comp} is the fluorescence intensity, which is achieved asymptotically upon complete binding at infinite lipid concentration. The results of F vs. $[L]$ were fitted to the above function to yield K_b and F_{comp}. Fig. 2 displays, as an example, the fluorescence spectra of HP3 in aqueous buffer solution and with increasing concentrations of lipid. The commonly observed red shift upon entering the lipid domain is seen in the figure, in which the peak wavelength shifts from 618 to 623 nm. This shift is accompanied by an amplification of the fluorescence spectrum. The inset in the figure shows data as analyzed by Eq. 1. The binding constants of the four hematoporphyrins to lecithin liposomes are presented in Table 1. It can be seen that the binding of the hematoporphyrin derivatives increases with the number of carbon atoms in the carboxylate chain. Increasing the number of carbon atoms in each carboxylate chain from two to seven, leads to a threefold increase in K_b.

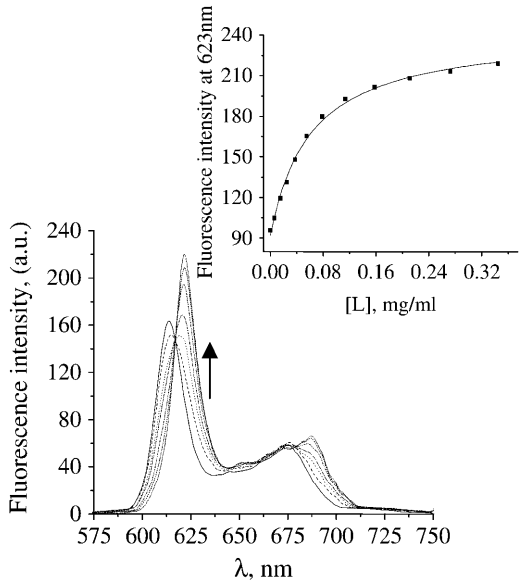

FIGURE 2 Fluorescence spectra [λ_{exc} = 402 nm] of 1 μM hematoporphyrin-IX (HP3) in water and in a suspension of lecithin liposomes at increasing concentrations of lipid (in these representative spectra: 0, 15, 37, 55, 113, 212, and 345 μg/ml). The arrow indicates the direction of change at increasing lipid concentrations. The intensity of the fluorescence at 626 nm is shown in the inset, together with the line, fitted according to Eq. 1.

TABLE 1 Binding constants (K_b) of hematoporphyrins to lecithin liposomes, their quenching constants (K_q) in liposomes by iodide, relative to the quenching in aqueous buffer solutions and singlet oxygen yields (Φ_Δ) in liposomes, relative to that of HP2

Porphyrin	K_b (mg/ml)$^{-1}$	K_q(lip)/K_q(buf)	Φ_Δ
HP2	15.4 ± 1.3	0.573 ± 0.072	1
HP3	16.2 ± 1.4	0.612 ± 0.083	1.042 ± 0.103
HP5	44.8 ± 3.2	0.301 ± 0.022	1.344 ± 0.129
HP7	45.2 ± 4.8	0.159 ± 0.093	1.437 ± 0.122

Comparative depths of the hematoporphyrin derivatives in liposomes

Quenching of the fluorescence of molecules with iodide ions (KI) is one of the simplest ways to obtain information about the relative vertical depth of membrane-bound fluorophores, including porphyrins, within membranes (Chalpin and Kleinfeld, 1983; Cranney et al., 1983; Barenholz et al., 1991; Moro et al., 1993; Vanesch et al., 1994; Lavi et al., 2002). Fluorescence quenching is associated with a quenching constant, K_q, which is obtained from the Stern-Volmer equation,

$$\frac{F_0}{F} = 1 + k_q\tau_0[Q] = 1 + K_q[Q], \quad (2)$$

where F_0 and F are fluorescence intensities in the absence and presence of the quencher, respectively, and $[Q]$ is the concentration of the quencher. To obtain K_q for each porphyrin derivative, F_0/F vs. $[Q]$ data were plotted, and fitted to Eq. 2 by a linear regression routine. Fig. 3 shows fluorescence quenching results of the hematoporphyrin analogs in buffer, and when bound to liposomes, together with the fitted Stern-Volmer lines. We employed in each case high enough lipid concentrations, to ensure that practically all the porphyrin was membrane-bound. For the comparison of quenching constants of the various analogs in liposomes to be indicative of their relative immersion depths in the bilayer, we contrast these quenching constants with the constant obtained in buffer only. The latter is thus indicative of the intrinsic quenching efficiency under homogeneous, isotropic conditions. Thus, any intrinsic parameters that affect the quenching efficiency, and that are not related to the vertical location in the lipid bilayer, are delineated. The results are listed in Table 1. As can be seen, as the number of carbon atoms in the carboxylate chains increases from two to seven, the ratio K_q(buf)/K_q(lip) decreases by approximately a factor of 4. We conclude that elongation of the alkyl carboxylate chains causes the sensitizer to penetrate and reside deeper within the lipid bilayer, and thus be less exposed to external quenching.

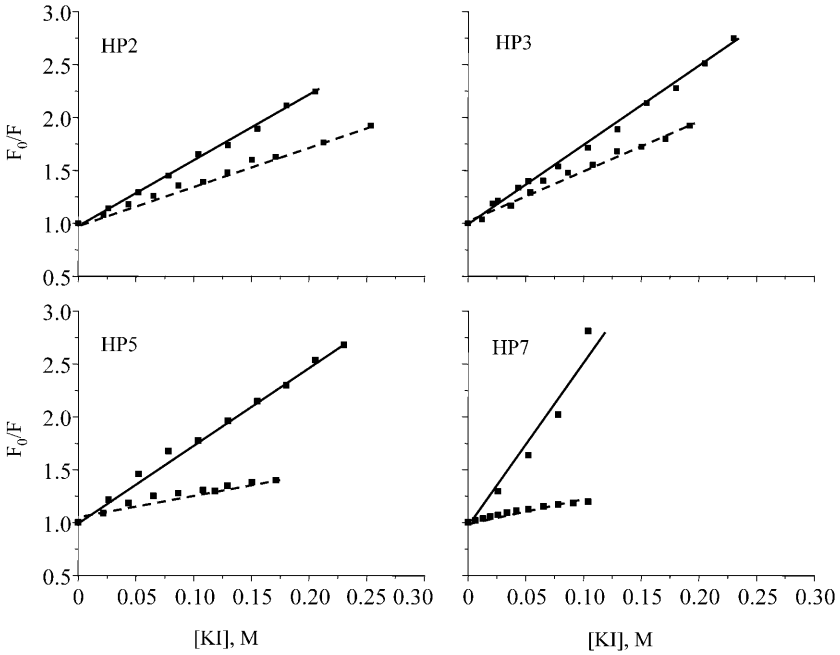

FIGURE 3 Stern-Volmer quenching plots of the hematoporphyrins (0.3 μM) in buffer solutions (*full lines*) and when bound to lecithin liposomes (0.5 mg lipid per ml, *dashed lines*). Fluorescence intensities were excited at 402 nm and measured at 626 nm.

Measurement of absolute depths of porphyrins in membranes by the parallax method

The parallax method enables the determination of the vertical depth of a fluorophore in a membrane bilayer, by the relative quenching that is observed with different membrane-bound quenchers, whose own depth is known. Equation 3 was developed for calculating the distance of the fluorophore from the center of the bilayer, Z_{cf} (Chattopadhyay and London, 1987),

$$Z_{cf} = \frac{\frac{1}{-\pi \times C} \times \ln\frac{F_1}{F_2} - L_{21}^2}{2L_{21}} + L_{C1}, \qquad (3)$$

where F_1 and F_2 are the fluorescence intensities of the fluorophore in the presence of a quencher that is located in shallow and deep vertical locations in the membrane, respectively; L_{21} is the vertical distance between the shallow and the deep quenchers; L_{c1} is the distance between the shallow quencher and the center of the bilayer; and C is the concentration of the quencher, in molecules per unit area. As quenchers, we employed 5-SLPC, 12-SLPC, and TempoPC, which were used also by London and co-workers (Kaiser and London, 1998a,b; Asuncion-Punzalan et al., 1998; Kachel et al., 1998). The distance of the nitroxide quenchers from the center of the bilayer was established as 19.5 Å for TempoPC, 12.15 Å for 5-SLPC, and 5.85 Å for 12-SLPC (Abrams and London, 1993). To calculate Z_{cf}, the pair of nitroxide labels whose quenching effect was the largest, indicating that they are, vertically, closest to the porphyrin, was used for the calculation. This model is based on the assumption that there is complete quenching of a fluorophore molecule if the quencher molecule is located within a critical distance, and there is no quenching when the distance is larger. At present, it is accepted that quenching by nitroxide, and by oxygen, is due to enhanced intersystem crossing caused by the paramagnetic quencher. Fig. 4 shows the distance of the PP analogs from the center of the bilayer. As can be seen from the figure, elongation of the alkyl carboxylate chain causes the sensitizer's location to be deeper within the membrane.

Photosensitization efficiencies

We used DMA as a singlet oxygen chemical trap, for the determination of relative singlet oxygen quantum yields. The disappearance of DMA's fluorescence, while the solution that includes the sensitizer is illuminated, followed first-order exponential decay kinetics, characterized by a kinetic rate constant, k_{DMA}.

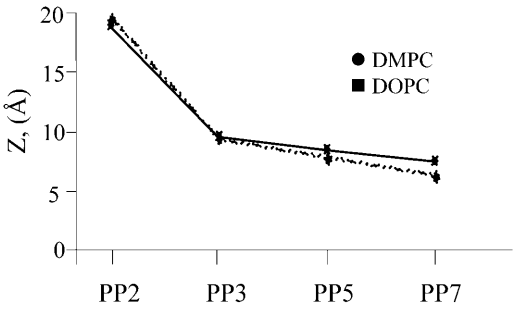

FIGURE 4 The distance of the protoporphyrins from the center of the bilayer, obtained by the parallax method, in liposomes composed of DMPC and DOPC.

The rate of absorption of photons by the sensitizer, k_{pho}, is given by the equation

$$k_{pho} = \frac{0.97 \times P \times (1 - 10^{-abs \cdot L})}{(0.1197/\lambda) \times V}, \quad (4)$$

where P is the irradiating laser power (in mW); *abs* is the absorbance, per cm, of the sensitizer at the wavelength of irradiation, λ; L is the length of the optical path of the laser beam in the sample; and V is volume of the sample (in ml). The factor 0.97 corrects for the reflection of the laser at the air/sample interface, by the Fresnel equations of reflection (Gross et al., 1993).

Singlet oxygen quantum yields, Φ_Δ, are proportional to the ratio of the rate of the target's disappearance and the rate of absorption of photons by the sensitizer, k_{DMA}/k_{pho}. The yields were calculated, relative to a standard sensitizer, HP3, whose yield was previously reported (Wilkinson et al., 1995) via the equation

$$\frac{\Phi_{\Delta,sens}}{\Phi_{\Delta,stand}} = \frac{\left(\frac{k_{DMA}}{k_{pho}}\right)_{sens}}{\left(\frac{k_{DMA}}{k_{pho}}\right)_{stand}}. \quad (5)$$

Singlet oxygen yields for the HP analogs are shown in Table 1. As can be seen from the table, the photosensitizing efficiency of the HP analogs, when bound to liposomes, increases with elongation of their alkyl carboxylate chains, up to >40%. To establish the validity of the observation of an apparent effect of depth on the efficiency of damage caused by singlet oxygen, we measured the yield in homogeneous solutions. The Φ_Δ of HP2, HP3, HP5, and HP7 in methanol were all 0.74 ± 0.04.

The effect of temperature on intra- and extramembranal fluorescence quenching

We measured the quenching constants of lecithin-bound hematoporphyrins in the temperature range 6°–40°C. As seen in Fig. 5, the effect of temperature is not very pronounced, exhibiting in most cases some trend of increase.

We studied the influence of temperature on the sensitizers' depth in the membrane, as measured by the parallax method. The experiments were carried out on PP analogs in liposomes composed of DMPC and DOPC. The results we obtained for the distances from the bilayer's center for PP3 in DMPC liposomes were 9.3, 8.9, and 8.7 Å, at 25°C, 35°C, and 45°C, respectively. The results for PP5 in DOPC liposomes were, for the same temperatures, 8.4, 8.3, and 8.3 Å. At these temperatures the lipid bilayers are in the fluid phase. These data clearly exhibit only a very small effect of temperature: for both porphyrins in both lipid membranes, increasing the temperature seems to move the porphyrins very slightly deeper into the bilayer. This trend appears to contrast the behavior that is inferred from the iodide quenching data, shown in Fig. 5.

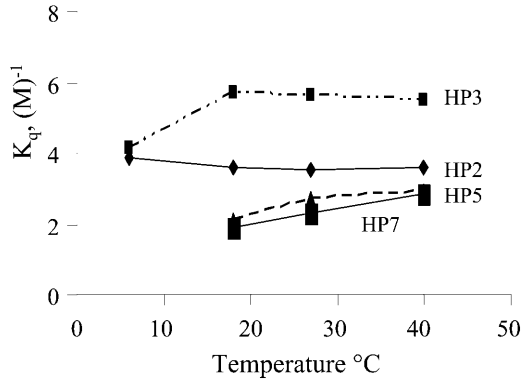

FIGURE 5 The effect of temperature on the Stern-Volmer iodide-quenching constants of the hematoporphyrins in lecithin liposomes.

The relative fluorescence quenching efficiencies of the HP and PP analogs by iodide in DMPC liposomes are depicted in Figs. 6 and 7, as a function of temperature. The temperature range spans from 7°C, where the DMPC bilayer is in the solid gel phase, up to 45°C, where the bilayer is in the liquid crystalline phase. We did not carry out parallax quenching below the phase transition temperature of DMPC liposomes. London and Feigenson showed that when liposomes are made of a mixed lipid composition containing similar spin-labeled phospholipids, phase separation occurs at low temperatures, forming a spin-labeled, lipid-rich liquid crystal phase and a spin-labeled, lipid-depleted gel phase (London and Feigenson, 1981; Ahmed et al., 1997).

DISCUSSION

The binding constants of the hematoporphyrin analogs increase with the number of carbon atoms in the carboxylate

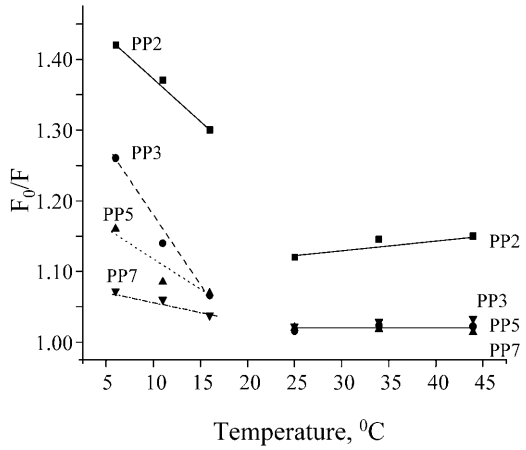

FIGURE 6 The effect of temperature on the fluorescence quenching efficiencies of the protoporphyrins by iodide in DMPC liposomes.

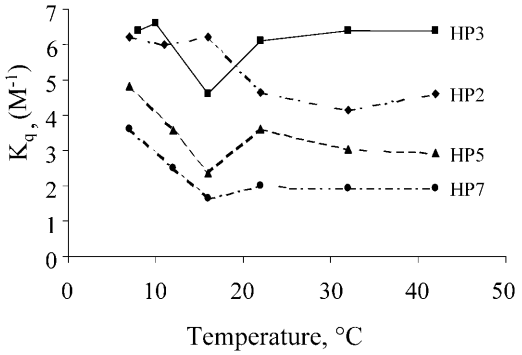

FIGURE 7 The effect of temperature on the Stern-Volmer iodide-quenching constants of the hematoporphyrins in DMPC liposomes.

chain. The lowest $K_b = 15.4 \pm 1.3$ (ml/mg lipid) belongs to HP2, increasing to 45.2 ± 4.8 (ml/mg lipid) for HP7. This effect is attributed to an increase in the hydrophobicity upon elongation of the alkyl chains. We have reported in a previous study that in the case of porphyrins that are similar in structure, the binding constants to liposomes exhibited a good linear correlation with the lipophilicity parameters logP and logD (Kepczynski et al., 2002). This effect was more pronounced for the protoporphyrins than for the analogous hematoporphyrins. In that study we reported that the calculated logP values for partitioning between water and *n*-octanol were 3.75, 4.69, 6.73, and 8.77 for HP2 to HP7, respectively, and 6.30, 7.27, 9.31, and 11.35 for the corresponding, more hydrophobic, protoporphyrins. The calculated logD values, which are more realistic by taking into consideration the deprotonation of carboxylic groups, were −1.44, −0.59, 1.69, 3.79; and 1.42, 2.01, 4.27, 6.37 for the two groups of molecules, respectively. The logD values of the hematoporphyrins were lower by 1–2.5 units than those of the protoporphyrins with similar length of carboxylate chains. This was observed for the calculated, as well as for the measured, logD results (Kepczynski et al., 2002). Similarly, the K_b values of the hematoporphyrins were 7–10 times smaller than for the corresponding protoporphyrins. This is readily explained on the basis of the higher hydrophobicity of protoporphyrin attributable to the two hydrophobic vinyl moieties, $-CH=CH_2$, compared with the more hydrophilic hydroxyl side groups of hematoporphyrin. One consequence of this is the contrast between the high binding constant of the more hydrophobic molecules and the slow kinetics leading to the equilibrium state. We think that the slow binding rate arises from the tendency of the hydrophobic molecules to aggregate in water. Thus, the hematoporphyrins took just minutes to reach binding equilibrium, whereas the protoporphyrins required much longer periods of shaking to equilibrate with the lipid phase. The formation of nonfluorescent aggregates was also reflected in a decrease of fluorescence intensity in aqueous solutions, upon changing from HP2 to HP7.

The results of fluorescence quenching of the porphyrins by iodide ions show that besides the stronger uptake of porphyrins with elongated side chains by liposomes, the bulk of the tetrapyrrole is located deeper in the membrane. As Fig. 3 and Table 1 demonstrate, the quenching efficiency of the hematoporphyrins that are located in liposomes decreases, relative to the quenching in buffer ($K_{q,lip}/K_{q,buf}$), as the chains lengthen. This is rationalized by the reasonable assumption that the molecules insert into the lipid bilayer down to the point that the charged carboxylates are anchored at the lipid/water interface. It has been shown in previous studies that porphyrins that are charged at their imino nitrogens do not partition into membranes, but deprotonation of the carboxylic moieties does not prevent partitioning but rather places them near the interface (Kepczynski and Ehrenberg, 2002). We chose iodide as a quencher since it usually does not produce static interactions. It is preferred as a quencher of membrane-bound fluorophores because it does not cause coagulation and disturbance to lyophils, and its quenching mechanism is not directional as with some other quenchers (Ford and Tollin, 1984), but rather isotropic. We did not encounter nonlinearities in the quenching experiments, as was observed by Ricchelli et al. (1988) when they quenched hematoporphyrins in micelles and liposomes by methylviologen or by anthraquinones. This indicates that the mechanism of quenching by iodide ions is purely collisional, due to ballistic penetration into the membrane, without formation of static interactions.

An interesting point to be observed in Fig. 3 is the trend of the quenching constants in buffer with chain length. The value K_q equals 6.5 M^{-1} for HP2, 7.1 M^{-1} for HP3, 7.5 M^{-1} for HP5, and 12 M^{-1} for HP7. This might be a result of an electrostatic repulsion between the approaching iodide ion and the charged carboxylates, that are located farther from the tetrapyrrole chromophore as the chains lengthen, and thus repel less the iodide and allow better quenching.

This important result, that the vertical displacement of the porphyrins is increased with elongation of the side chains, was observed earlier with the series of protoporphyrins (Lavi et al., 2002). The iodide quenching experiments lead, however, only to qualitative information about the depth location, as evidenced from the accessibility to external quenching. In addition, as explained above, it is necessary to compare the effect of iodide quenching in membranes to that obtained in aqueous solution. This, however, is a difficult task when the water solubility is extremely low, as is the case with protoporphyrins. To evaluate quantitatively, in Ångstroms, the depth of the porphyrins, we utilized the parallax method on the series of protoporphyrins. The distance of the effective center of the protoporphyrin fluorophore from the midpoint of the bilayer is shown in Fig. 4, for DOPC and DMPC liposomes. The location changes from ~19 Å for PP2, i.e., the fluorophore is practically near the water interface, to ~7 Å for PP7.

As the chromophoric part of the molecule is inserted deeper in the membrane, singlet oxygen is produced by photosensitization at a greater depth. Its longer path of diffusion results in a more efficient photodamaging process of a membrane-localized target, such as DMA. This was indeed observed when we measured the apparent yield of singlet-oxygen production, Φ_Δ. The results that are tabulated in Table 1 show a 44% increase upon changing from HP2 to HP7. It is unlikely that this increase is due to a depth-dependent increase in the efficiency of a singlet oxygen pathway over the pathway of other reactive oxygen species, since the yield of the latter is known to be very low. These results suggest the possibility of chemically modifying an existing photosensitizer in a way that will place it deeper in the membrane. This in turn will enhance its photosensitizing efficiency for wreaking damage to singlet oxygen targets that exist inside the membrane.

We have studied the influence of temperature on the localization of the hematoporphyrins in the membrane, by following the effect of temperature on fluorescence quenching processes. As seen in Fig. 5, there was practically no temperature effect on the quenching efficiency of HP2 by iodide in lecithin liposomes, K_q being $3.6 \pm 0.1\ M^{-1}$ over the range 6–40°C. There is a mixed effect in the case of HP3 and some increase of quenching in HP5 and HP7, changing K_q from 1.9 to $2.86\ M^{-1}$. The lack of temperature effect with HP2 is explainable on the basis of this molecule lying close to the lipid/water interface. Its carboxylates are anchored at this interface and the tetrapyrrole ring is also very close to it. HP5 and HP7 sink deeper into the lipid layer, because of the longer alkyl spacers.

The observed effect of temperature on the quenching could arise either from a vertical displacement outwards as the temperature increases, or because of deeper penetration of the iodide ions into the lipid phase at higher temperatures. To discriminate between these two possibilities we reverted to the parallax method. We measured the quenching of HP5 and HP7 in lecithin liposomes, in the temperature range 25–45°C, i.e., above the solid-to-liquid phase transition temperature. The quenching efficiency by each of the three spin-label quenchers was identical, within 3%, at the different temperatures, indicating very small, if any, temperature-dependent displacement of the porphyrins, as long as the physical phase of the lipid is not changed. This phenomenon was also observed when we measured the depth of PP3 and PP5 in DOPC and DMPC liposomes, in the temperature range 25–45°C, i.e., above the solid-to-liquid phase transition. Thus, the small effect of temperature on quenching of lecithin-bound porphyrins by iodide, that was seen in Fig. 5, can be attributed to the temperature effect on the penetration depth of iodide ions into the membrane.

In contrast to the former observations, a strong temperature effect is observed when the temperature range spans the solid-to-liquid phase transition. As can be seen in Figs. 6 and 7, quenching of hematoporphyrins and protoporphyrins by extramembranal iodide exhibits a sharp breaking point at the phase-transition temperature. Above this temperature, when in the liquid phase, there is hardly any dependence of the quenching efficiency on temperature, as was discussed above. However, when the temperature is lowered below this point, the efficiency of quenching increases as the temperature decreases. Recalling the previous discussion about the effect that temperature probably has on the kinetic penetration of iodide into the membrane phase, we might expect a very small lowered efficiency of quenching as the temperature decreases, due to lower kinetic energy of the iodide ions. Thus, the trend of increased quenching that is observed in Figs. 6 and 7 in the range of 5°–20°C is even more outstanding. We have observed, in a previous study (Lavi et al., 2002), that ''freezing'' liposomes to the solid gel phase tends to extrude a porphyrin toward the lipid/water interface, whereas incorporation of cholesterol in the membrane pushed the porphyrin deeper into the lipid bilayer.

CONCLUSION

The present study demonstrates that the vertical localization of a photosensitizer in a lipid membrane can be modulated by inserting spacer moieties into the molecular structure, while anchoring one end of the molecule at the lipid/water interface. The porphyrins with a longer spacer generate singlet oxygen, via photosensitization, at a deeper point, which in turn results in greater photodamage caused to a membrane-residing singlet oxygen target. The vertical location can be assessed by iodide fluorescence quenching and measured by the parallax method. The depth of the porphyrin's core in the membrane is not affected by the temperature when the membrane is in the liquid phase. However, upon changing to the solid phase, lowering the temperature buoys up, or rather extrudes, the hemato- and protoporphyrins toward the water interface.

The depth of membrane-bound proteins and peptides is known to have implications to their activity in the membrane (Shinitzky, 1984). This, however, is not the case with small molecules that partition into membranes. The numerous publications by the group of London, some of which were referenced in this article, are demonstrations of the assessment of the depth of small molecules in membranes. However, the results presented in this manuscript, together with those in our previous article (Lavi et al., 2002), are unique in presenting not mere information on the depth of small molecules in membranes, but clearly pointing to the practical relevance of this depth to the activity of this class of small molecules in the membrane.

Modifications of the structure of other membrane-binding photosensitizers, similar to those done to the hemato- and protoporphyrins in this study, could also place them deeper in the lipid bilayer. Consequently, an additional important criterion for choosing and designing a new photosensitizer can emerge. One should indeed aim for a high quantum yield

for generation of singlet oxygen, an absorption band located at long wavelengths to enable deeper light penetration, and good uptake by the cells' membranes and selectivity of binding to cancer cells. Now, however, deep vertical penetration of the sensitizer in the membrane could also be required. This would increase the photosensitized damage that is exerted, without restricting the above-mentioned criteria that have been selected. We are currently testing the findings of this study in cells, which are naturally more complex systems because they contain various natural chemical quenchers of singlet oxygen.

We thank Professor Erwin London from the State University of New York at Stony Brook for his assistance with the application of the parallax method.

We acknowledge the kind and generous support of the United States-Israel Binational Science Foundation, Jerusalem, Israel (grant 2002383 to B.E., A.A.F., and K.M.S.), and the National Institutes of Health (grant HL-22252 to K.M.S.). We also acknowledge the support of the Michael David Falk Chair in Laser Phototherapy and the Ethel and David Resnick Chair in Active Oxygen Chemistry.

REFERENCES

Abrams, F. S., and E. London. 1993. Extension of the parallax analysis of membrane penetration depth to the polar region of model membranes—use of fluorescence quenching by a spin-label attached to the phospholipid polar headgroup. *Biochemistry.* 32:10826–10831.

Ackroyd, R., C. Kelty, N. Brown, and M. Reed. 2001. The history of photodetection and photodynamic therapy. *Photochem. Photobiol.* 74:656–669.

Ahmed, S. N., D. A. Brown, and E. London. 1997. On the origin of sphingolipid/cholesterol-rich detergent-insoluble cell membranes: physiological concentrations of cholesterol and sphingolipid induce formation of a detergent- insoluble, liquid-ordered lipid phase in model membranes. *Biochemistry.* 36:10944–10953.

Allen, C. M., W. M. Sharman, and J. E. Van Lier. 2001. Current status of phthalocyanines in the photodynamic therapy of cancer. *J. Porphyr. Phthalocyan.* 5:161–169.

Asuncion-Punzalan, E., K. Kachel, and E. London. 1998. Groups with polar characteristics can locate at both shallow and deep locations in membranes: the behavior of dansyl and related probes. *Biochemistry.* 37:4603–4611.

Barenholz, Y., T. Cohen, R. Korenstein, and M. Ottolenghi. 1991. Organization and dynamics of pyrene and pyrene lipids in intact lipid bilayers. Photo-induced charge transfer processes. *Biophys. J.* 60:110–124.

Berg, K., and J. Moan. 1997. Lysosomes and microtubules as targets for photochemotherapy of cancer. *Photochem. Photobiol.* 65:403–409.

Bonnett, R. 2002. Progress with heterocyclic photosensitizers for the photodynamic therapy (PDT) of tumours. *J. Heterocyclic Chem.* 39: 455–470.

Borochov, H., and M. Shinitzky. 1976. Vertical displacement of membrane proteins mediated by changes in microviscosity. *Proc. Natl. Acad. Sci. USA.* 73:4526–4530.

Chalpin, D. B., and A. M. Kleinfeld. 1983. Interaction of fluorescent quenchers with the *n*-(9-anthroyloxy) fatty acid membrane probes. *Biochim. Biophys. Acta.* 731:465–474.

Chattopadhyay, A., and E. London. 1987. Parallax method for direct measurement of membrane penetration depth utilizing fluorescence quenching by spin-labeled phospholipids. *Biochemistry.* 26:39–45.

Corey, E. J., and W. C. Taylor. 1964. Study of the oxidation of organic compounds by externally generated singlet oxygen molecules. *J. Am. Chem. Soc.* 86:3881–3882.

Cranney, M., R. B. Cundall, G. R. Jones, J. T. Richards, and E. W. Thomas. 1983. Fluorescence lifetime and quenching studies on some interesting diphenylhexatriene membrane probes. *Biochim. Biophys. Acta.* 735: 418–425.

DeRosa, M. C., and R. J. Crutchley. 2002. Photosensitized singlet oxygen and its applications. *Coord. Chem. Rev.* 233:351–371.

Dougherty, T. J. 2002. An update on photodynamic therapy applications. *J. Clin. Laser Med. Surg.* 20:3–7.

Ehrenberg, B. 1992. Assessment of the partitioning of probes to membranes by spectroscopic titration. *J. Photochem. Photobiol. B Biol.* 14:383–386.

Ehrenberg, B., E. Gross, Y. Nitzan, and Z. Malik. 1993. Electric depolarization of photosensitized cells—lipid vs. protein alterations. *Biochim. Biophys. Acta.* 1151:257–264.

Ehrenberg, B., J. L. Anderson, and C. S. Foote. 1998. Kinetics and yield of singlet oxygen photosensitized by hypericin in organic and biological media. *Photochem. Photobiol.* 68:135–140.

Fabris, C., G. Valduga, G. Miotto, L. Borsetto, G. Jori, S. Garbisa, and E. Reddi. 2001. Photosensitization with zinc (II) phthalocyanine as a switch in the decision between apoptosis and necrosis. *Cancer Res.* 61: 7495–7500.

Fischkoff, S., and J. M. Vanderkooi. 1975. Oxygen diffusion in biological and artificial membranes determined by the fluorochrome pyrene. *J. Gen. Physiol.* 65:663–676.

Ford, W. E., and G. Tollin. 1984. Chlorophyll photosensitized electron transfer in phospholipid bilayer vesicle systems: effects of cholesterol on radical yields and kinetic parameters. *Photochem. Photobiol.* 40: 249–259.

Gross, E., B. Ehrenberg, and F. M. Johnson. 1993. Singlet oxygen generation by porphyrins and the kinetics of 9,10-dimethylanthracene photosensitization in liposomes. *Photochem. Photobiol.* 57:808–813.

Holmes, R. T. 1997. Synthetic studies of poly-pyrrolic macrocycles. PhD dissertation. University of California, Davis, CA.

Kachel, K., E. Asuncion-Punzalan, and E. London. 1995. Anchoring of tryptophan and tyrosine analogs at the hydrocarbon polar boundary in model membrane liposomes: parallax analysis of fluorescence quenching induced by nitroxide-labeled phospholipids. *Biochemistry.* 34:15475–15479.

Kachel, K., E. Asuncion-Punzalan, and E. London. 1998. The location of fluorescence probes with charged groups in model membranes. *Biochim. Biophys. Acta Biomembr.* 1374:63–76.

Kaiser, R. D., and E. London. 1998a. Determination of the depth of BODIPY probes in model membranes by parallax analysis of fluorescence quenching. *Biochim. Biophys. Acta Biomembr.* 1375:13–22.

Kaiser, R. D., and E. London. 1998b. Location of diphenylhexatriene (DPH) and its derivatives within membranes: comparison of different fluorescence quenching analyses of membrane depth. *Biochemistry.* 37:8180–8190.

Kepczynski, M., and B. Ehrenberg. 2002. Interaction of dicarboxylic metalloporphyrins with liposomes. The effect of pH on membrane binding revisited. *Photochem. Photobiol.* 76:486–492.

Kepczynski, M., R. P. Pandian, K. M. Smith, and B. Ehrenberg. 2002. Do liposome-binding constants of porphyrins correlate with their measured and predicted partitioning between octanol and water? *Photochem. Photobiol.* 76:127–134.

Kessel, D., and Y. Luo. 2001. Intracellular sites of photodamage as a factor in apoptotic cell death. *J. Porphyr. Phthalocyan.* 5:181–184.

Lavi, A., H. Weitman, R. T. Holmes, K. M. Smith, and B. Ehrenberg. 2002. The depth of porphyrin in a membrane and the membrane's physical properties affect the photosensitizing efficiency. *Biophys. J.* 82:2101–2110.

London, E., and G. W. Feigenson. 1981. Fluorescence quenching in model membranes. An analysis of the local phospholipid environments

of diphenylhexatriene and gramicidin A′. *Biochim. Biophys. Acta*. 649: 89–97.

MacDonald, I. J., and T. J. Dougherty. 2001. Basic principles of photodynamic therapy. *J. Porphyr. Phthalocyan*. 5:105–129.

Moan, J. 1990. On the diffusion length of singlet oxygen in cells and tissue. *J. Photochem. Photobiol. B Biol*. 6:343–344.

Moor, A. C. E. 2000. Signaling pathways in cell death and survival after photodynamic therapy. *J. Photochem. Photobiol. B Biol*. 57:1–13.

Moro, F., F. M. Goni, and M. A. Urbaneja. 1993. Fluorescence quenching at interfaces and the permeation of acrylamide and iodide across phospholipid bilayers. *FEBS Lett*. 330:129–132.

Oleinick, N. L., R. L. Morris, and T. Belichenko. 2002. The role of apoptosis in response to photodynamic therapy: what, where, why, and how. *Photochem. Photobiol. Sci*. 1:1–21.

Paardekooper, M., P. J. A. Van den Broek, A. W. De Bruijne, J. G. R. Elferink, T. M. A. R. Dubbelman, and J. Van Steveninck. 1992. Photodynamic treatment of yeast cells with the dye toluidine blue: all-or-none loss of plasma membrane barrier properties. *Biochim. Biophys. Acta*. 1108:86–90.

Pandey, R. K. 2000. Recent advances in photodynamic therapy. *J. Porphyr. Phthalocyan*. 4:368–373.

Ricchelli, F., D. Stevanin, and G. Jori. 1988. Porphyrin-liposome interactions: influence of the physico-chemical properties of the phospholipid bilayer. *Photochem. Photobiol*. 48:13–18.

Roslaniec, M., H. Weitman, D. Freeman, Y. Mazur, and B. Ehrenberg. 2000. Liposome binding constants and singlet oxygen quantum yields of hypericin, tetrahydroxy helianthrone and their derivatives: studies in organic solutions and in liposomes. *J. Photochem. Photobiol. B Biol*. 57:149–158.

Schweitzer, C., and R. Schmidt. 2003. Physical mechanisms of generation and deactivation of singlet oxygen. *Chem. Rev*. 103:1685–1757.

Shinitzky, M. 1984. Membrane fluidity and cellular function. *In* Physiology of Membrane Fluidity, Vol. 1. M. Shinitzky, Editor. CRC Press, Boca Raton, FL. 1–51.

Smith, K. M. 2000. Strategies for the syntheses of octaalkylporphyrin systems. *In* The Porphyrin Handbook, Vol. 1. K. M. Kadish, K. M. Smith, and R. Guilard, editors. Academic Press, Boston, MA. 25–28.

Smith, R. P., and S. M. Hahn. 2002. Photodynamic therapy. *Curr. Prob. Cancer*. 26:67–108.

Usui, Y. 1973. Determination of quantum yield of singlet oxygen formation by photosensitization. *Chem. Lett*. 743–744.

Vanesch, J. H., M. C. Feiters, A. M. Peters, and R. J. M. Nolte. 1994. UV-vis, fluorescence, and EPR studies of porphyrins in bilayers of dioctadecyldimethylammonium surfactants. *J. Phys. Chem*. 98:5541–5551.

Wilkinson, F., and J. G. Brummer. 1981. Rate constants for the decay and reactions of the lowest electronically exited singlet state of molecular oxygen in solution. *J. Phys. Chem. Ref. Data*. 10:809–999.

Wilkinson, F., W. P. Helman, and A. B. Ross. 1995. Rate constants for the decay and reactions of the lowest electronically excited singlet state of molecular oxygen in solution. An expanded and revised compilation. *J. Phys. Chem. Ref. Data*. 24:663–1021.